Antitumor effect of COOH-terminal polypeptide of human TERT is associated with the declined expression of hTERT and NF-κB p65 in HeLa cells

XIAN WU[1,2], JIASHENG CHEN[1,2], YING CAO[1,2], BAOPING XIE[1,2], HONGWEI LI[3], PINGZHENG ZHOU[1,2], YUCHANG QIU[1,2] and JIANXIN PANG[1,2]

[1]Center for Drug Evaluation and Research, and [2]Guangdong Provincial Key Laboratory of New Drug Screening, School of Pharmaceutical Sciences, and [3]School of Biotechnology, Southern Medical University, Baiyun, Guangzhou, Guangdong 510515, P.R. China

Received May 27, 2015; Accepted July 3, 2015

DOI: 10.3892/or.2015.4298

Abstract. Human telomerase reverse transcriptase (hTERT) plays an important role in the development of tumors and has been investigated as a potent target for anticancer therapy. In the present study, we constructed a recombinant adenovirus, Ad-EGFP-C197 which was capable of expressing COOH-terminal polypeptide of hTERT (amino acid 936-1,132, termed as C197 for the reason that it contains 197 amino acids). Infection of HeLa cells with Ad-EGFP-C197 suppressed the activity of telomerase, decreased the expression of hTERT and NF-κB p65, and induced rapid growth delay and apoptosis of HeLa cells *in vitro*. In nude mice xenografted with HeLa tumors, injection of Ad-EGFP-C197 into the tumor nodule significantly slowed tumor growth and promoted tumor cell apoptosis, as well as reduced the expression of NF-κB p65 in tumor tissues. In the present study, we suggest that the antitumor effect of C197 is associated with the declined expression of hTERT and NF-κB p65. Our results highlight the potential of C197 in tumor therapy.

Introduction

Telomeres are the ends of linear chromosomes in eukaryotic cells and are characterized by the TTAGGG repeats (1) that are bound by the shelterin complex (2). Telomeric DNA shrinks with each cellular division due to incomplete replication of TTAGGG repeats, which eventually results in DNA damage and replicative senescence (3). Telomerase is a particular ribonucleoprotein complex which specifically adds TTAGGG repeats to the ends of eukaryotic chromosomes, thus counteracts the shortening of telomeric DNA during cell division. The activity of telomerase is not detected in most human somatic cells (4). However, telomerase is reactivated in vast majority of human cancer cells (5) and plays a critical role in the progression of human cancer (6). Recently telomerase has been found to exert extra-telomeric effects via the modulation of NF-κB (7,8) and Wnt/β-catenin signaling pathways (9,10). These non-canonical functions are associated with the development and progression of human cancer. In fact, telomerase has been investigated as a potent target for anticancer therapy (11).

The major components of human telomerase are tolemerase RNA (hTR) and telomerase reverse transcriptase (hTERT). While hTR subunit serves as a template, hTERT subunit catalyzes the elongation of telomeric DNA. Three main structural domains of hTERT have been identified: NH_2 terminus that binds DNA and RNA, central catalytic RT region and a short COOH terminus (12). Although the function of COOH terminus is the least-characterized, it has been found to mediate the nuclear translocation of telomerase (13) and is essential for the *in vivo* activity of human telomerase (14). Recent studies showed that ectopic expression of C27 (amino acid 882-1,132 of hTERT) reduces the growth and tumorigenicity of tumor cells (15-19) and sensitizes tumor cells to 5-fluorouracil-induced growth inhibition and apoptosis (20). C27 does not affect telomerase activity. The unclearly illustrated mechanisms include the induction of telomere dysfunction (15), triggering of apoptosis signal and reduction of angiogenesis in tumor tissue (16), as well as involvement of immune responses (18).

In the present study, a novel COOH-terminal polypeptide (C197, amino acid 936-1,132) of hTERT was overexpressed in HeLa cells using recombinant adenovirus Ad-EGFP-C197. Ectopic expression of C197 was found to induce growth delay and promotes apoptosis of HeLa cells *in vitro,* and in nude mice. Furthermore, C197 suppressed the telomerase activity, as well as downregulated the expression of hTERT and NF-κB p65 in HeLa cells, demonstrating that the antitumor

Correspondence to: Professor Jianxin Pang or Dr Yuchang Qiu, Center for Drug Evaluation and Research, School of Pharmaceutical Sciences, Southern Medical University, 1023-1063 South Shatai Road, Baiyun, Guangzhou, Guangdong 510515, P.R. China
E-mail: pjx@smu.edu.cn
E-mail: qiuyuchang2013@163.com

Key words: human telomerase reverse transcriptase, COOH terminus, antitumor, HeLa cells, NF-κB p65

effect of C197 was associated with the reduced expression of hTERT and NF-κB p65.

Materials and methods

Ethics statement. All animal protocols conformed to the EU guidelines (2010/63/EU) and other EU recommendations, and were conducted with the approval of the Ethics Committee of Animal Experiments, Southern Medical University. All surgery was performed under sodium pentobarbital anesthesia, and every effort was made to minimize suffering.

Cell culture. HEK-293 (CRL-1573) and HeLa (CCL-2) cell lines were obtained from American type culture collection (ATCC; Manassas, VA, USA). Cells were cultivated in Dulbecco's modified Eagle's medium (DMEM) supplemented with 10% fetal bovine serum (FBS) (both from Gibco, USA) plus 100 U/ml penicillin and 100 μg/ml streptomycin (Sigma, USA) at 37˚C in a humidified atmosphere containing 5% CO_2.

Construction of Ad-EGFP-C197. The cDNA encoding C197 (hTERT amino acid 936-1,132) was synthesized by Sangon Biotech (Shanghai, China), and was identified by sequencing. A 6-histidine (6-His)-tag was added to the N-terminus of C197 cDNA to facilitate the detection of C197 protein. The AdEasy Vector system was used for the construction of recombinant adenovirus Ad-EGFP-C197. The construction, preparation and titration of Ad-EGFP-C197 were conducted as previously described (21), with the substitution of 6-His-C197 cDNA for AT2R cDNA. The foreign genes 6-His-C197 and enhanced green fluorescent protein (EGFP) were driven by a separate cytomegalovirus (CMV) promoter within the recombinant Ad-EGFP-C197. The mock adenovirus Ad-CMV-EGFP was prepared as previously described (21).

Detection of the expression of C197 in HeLa cells. Cells ($2x10^5$/well) were seeded into 6-well tissue culture plates (Corning, Shanghai, China). The following day, cells were infected with Ad-EGFP-C197 [multiplicity of infection (MOI) of 100]. Forty-eight hours after infection, cells were subject to the detection of C197 protein using anti-6-His antibody by western blotting as described below.

Determination of the sub-cellular localization of C197. HeLa cells ($1x10^5$) were cultivated in a 10 mm glass bottom culture dish (Corning). The following day, cells were infected with Ad-EGFP-C197 (MOI of 100). At the time point of 24 or 48 h after infection, cells were washed 3 times with phosphate-buffered saline (PBS), then fixed in 4% paraformaldehyde for 15 min, followed by the incubation with 1% BSA (Sigma) for 30 min. Next, cells were incubated with primary antibody against 6-His-tag (mouse monoclonal IgG, 1:500 dilution; sc-57598; Santa Cruz Biotechnology, Santa Cruz, CA, USA) at 37˚C for 1 h, washed with PBS and incubated with TRITC-coupled secondary antibody (goat polyclonal against mouse IgG, 1:100 dilution; BS11502; Bioworld Technology) for 1 h at room temperature. Cell nuclei were counterstained by phenylindole dihydrochloride (DAPI) (Sigma) for 5 min. After several washes with PBS, cells were examined under a confocal microscope (Nikon, Japan).

In vitro proliferation and apoptosis assay. For the cell proliferation assay, HeLa cells ($1x10^4$ cells/well) were seeded in 96-well plates (Corning). The following day, cells were infected with recombinant adenovirus Ad-EGFP-C197 or mock adenovirus Ad-EGFP (MOI of 100). Cells were cultivated for 7 days after infection. On each day cell viability was examined by MTT (Sigma) method using a Multiskan microplate reader (Benchmark Plus; Bio-Rad, USA).

For *in vitro* apoptosis assay, HeLa cells ($1x10^5$ cells/well) were seeded in 6-well plates (Corning). The following day, cells were infected with Ad-EGFP-C197 or Ad-EGFP (MOI of 100). Cells were cultivated for 3 days after infection. Each day cell apoptosis was detected using Annexin V-PE apoptosis detection kit I (BD Biosciences, USA) according to the manufacturer's instructions, and analyzed by flow cytometry (Bio-Rad) within 1 h.

Telomerase activity assay. HeLa cells ($1x10^5$ cells/well) were seeded into 6-well plates (Corning). The following day, cells were infected with Ad-EGFP-C197 or Ad-EGFP (MOI of 100). Forty-eight hours after infection, cell lysates were prepared and telomerase activity was determined using a TRAPeze® telomerase detection kit (S7700; Millipore, Billerica, MA, USA) as described in the manufacturer's instructions. Briefly, protein was extracted from cells and suspended in 1X CHAPS in a concentration of 700 ng/μl. PCR was performed in 50 μl reaction system (including 2 μl protein solution). Amplification reactions were performed for 30 cycles of 94˚C for 30 sec, 59˚C for 30 sec and 72˚C for 10 min. Products were separated by electrophoresis on 12.5% polyacrylamide gels, stained with EB for 30 min and scanned with a gel documentation system (Bio-Rad).

Detection of the expression of hTERT and NF-κB p65. HeLa cells ($1x10^5$ cells/well) were seeded into 6-well plates (Corning). The following day, cells were infected with Ad-EGFP-C197 or Ad-EGFP (MOI of 100). Forty-eight hours after infection, cell lysates were prepared to detect the expression of hTERT. For the detection of NF-κB p65, TNF-α (PeproTech, USA) was added to the medium (final concentration 10 ng/ml) and cells were cultivated for another 12 h. Cells were then collected to prepare cell lysates. The expression of hTERT and NF-κB p65 were detected by western blotting as described below.

Western blot analysis. Western blotting was performed according to standard protocols. Briefly, total protein was extracted from the cells by repeated freezing and thawing, or from tumor tissues by homogenization, and was quantified using the Bradford method. Samples were separated by SDS-PAGE and transferred onto a polyvinylidene fluoride (PVDF) membrane (Millipore) using Mini Trans-Blot (Bio-Rad). The membrane was blocked with 5% non-fat dry milk (Sigma) and incubated with primary antibodies, followed by the incubation with horseradish peroxidase (HRP)-conjugated secondary antibodies. The film was developed using the enhanced chemiluminescence (ECL) kit (Vazyme, Nanjing, China). Primary antibodies included mouse monoclonal antibodies (IgG) against 6-his-tag (1:500 dilution, sc-57598)/human GAPDH

(1:500 dilution, sc-365062)/human β-actin (1:500 dilution, sc-130301)/hTERT (1:100 dilution, sc-393013) (all from Santa Cruz Biotechnology), and rabbit monoclonal IgG against human NF-κB p65 (1:1,000 dilution, #8242; Cell Signaling Technology). The secondary antibodies used were HRP-conjugated goat polyclonal antibody against mouse IgG (1:5,000 dilution, BS12478) and HRP-conjugated goat polyclonal antibody against rabbit IgG (1:500 dilution, BS13278) (both from Bioworld Technology).

Animal studies. Male athymic nude mice (BALB/c-nu/nu) aged 4-6 weeks (Center of Laboratory Animals, Southern Medical University, Guangzhou, China) were housed in sterile cages with a 12:12 h light-dark cycle. Animals were fed autoclaved chow and water *ad libitum*. The tumors were established by subcutaneous injection of $1x10^7$ HeLa cells into the right flank of each mouse. When the tumor nodules reached 5-6 mm in diameter, mice were randomly divided into two groups of six mice. Each mouse received intratumor injection of Ad-EGFP-C197 or Ad-EGFP ($1x10^9$ pfu) twice a week for 4 weeks. Animals were observed for one week after the last injection. Tumor volumes were determined once a week by measuring in two dimensions and calculated as tumor volume = length x $(width)^2/2$ (22). At the end of the experiment, mice were sacrificed with sodium pentobarbital and tumor nodules were separated and weighed. Tumor tissues were subjected to TUNEL assay and immunohistochemistry analysis, and a fraction was homogenized for protein extraction and immunodetection of β-actin and 6-His-C197 by western blotting, as previously described.

TUNEL assay. Tumor tissues were fixed with 4% paraformaldehyde (Sigma) and were embedded in paraffin (Sigma). After dehydration, tissue sections (6-μm thick) were prepared and mounted on polylysine (Sigma) coated slides. Sections were then subject to deparaffinization and rehydration, followed by the microwave antigen retrieval with citric acid. TUNEL assay was conducted using the DeadEnd Colorimetric TUNEL System (Promega, Beijing, China) as described in the manufacturer's instructions. Stained sections were analyzed with a light microscope (Nikon). At least 3-high magnification fields were examined in each section (500 cells altogether), and the apoptotic index (AI) was calculated as the percentage of TUNEL-positive cells.

Immunohistochemistry analysis. Tissue sections were prepared as described above. After incubation with 3% H_2O_2 for 10 min and blocking with 5% BSA for 30 min, sections were incubated with primary antibody against NF-κB p65 (rabbit monoclonal IgG, 1:800 dilution, #8242; Cell Signaling Technology) for 12 h at 4˚C, followed by the incubation with HRP-conjugated goat polyclonal antibody against rabbit IgG (1:500 dilution, BS13278, Bioworld Technology) for 30 min at 37˚C. Next, 3,3'-diaminobenzidine (DAB; Sigma) was added to visualize the brown color. Finally, sections were counterstained with hematoxylin to show cell nuclei and examined with a light microscope (Nikon). The total integrate optical density (IOD) and total area of each section was determined with an Image-Pro Plus 6.0 software. The mean optical density (MOD) was employed to show the relative amount of p65 protein in each section using the following formula: mean optical density = total IOD/total area.

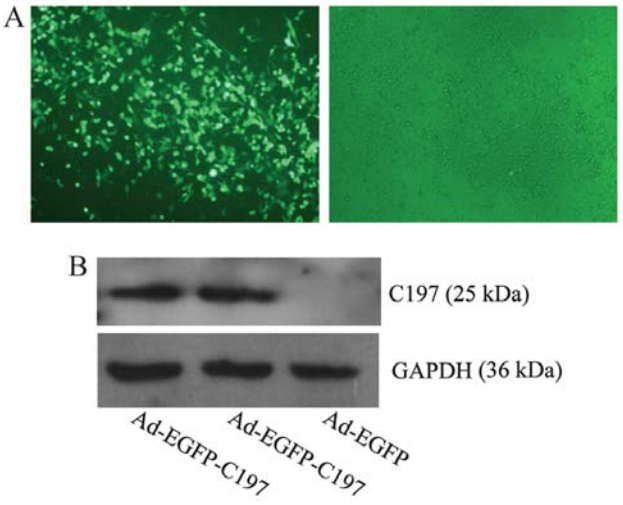

Figure 1. Ectopic expression of C197 in HeLa cells. (A) HeLa cells infected with Ad-EGFP-C197 (left, green fluorescence was shown; right, green fluorescence was not shown). Magnification, x100. (B) The expression of C197 protein in HeLa cells was confirmed by western blotting. GAPDH was used as an internal control.

Statistical analysis. Data are represented as mean ± standard deviation (SD). All statistical analyses were carried out using SPSS 13.0 (IBM, USA). Differences between groups were assessed using independent samples t-test and were considered to indicate a statistically significant result when the P-value was <0.05.

Results

Expression and sub-cellular localization of C197 in HeLa cells. As shown in Figs. 1 and 2, high level expression of C197 was achieved in HeLa cells by the infection of Ad-EGPF-C197. Within the first 24 h after infection, C197 accumulated predominantly in the cytoplasm, and appeared in the cell nucleus 48 h after infection (Fig. 2) demonstrating that C197 was capable of entering the nucleus.

Ad-EGFP-C197 induces growth delay and apoptosis of HeLa cells in vitro. We next evaluated the effect of C197 on the proliferation of HeLa cells. The results in MTT assay showed that Ad-EGFP-C197 significantly inhibited the proliferation of cells [optical density (OD) value, 1.17±0.20, 1.18±0.12, 1.44±0.06 and 1.68±0.10 at the 4, 5, 6 and 7 days after infection, respectively] compared to Ad-EGFP (OD value, 1.50±0.20, 1.72±0.28, 2.21±0.61 and 2.48±0.69 at the 4, 5, 6 and 7 days after infection, respectively, P<0.05 or P<0.01, Fig. 3A).

We further assayed the apoptosis rate of cells. Apoptotic rate was calculated using the following formula: apoptotic rate = (cells undergoing apoptosis and cells in end-stage apoptosis)/total cells. Ad-EGFPC197 induced a higher apoptosis rate (9.36±2.32, 25.03±4.00 and 38.07±2.59% at 24, 48 and 72 h after infection, respectively) compared to Ad-EGFP (4.53±0.59, 5.24±0.68 and 10.33±0.40% at 24, 48 and 72 h

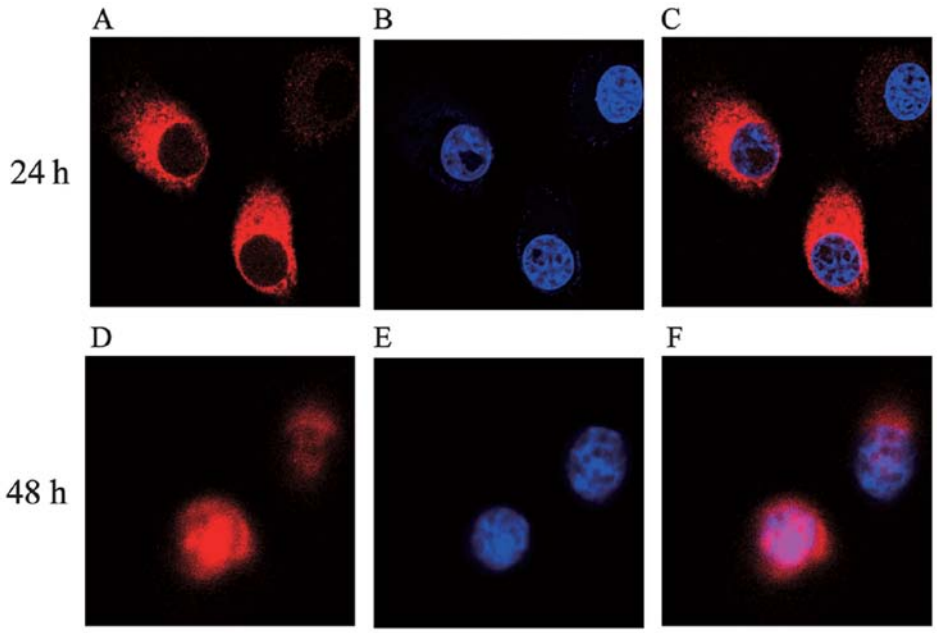

Figure 2. Sub-cellular localization of C197. C197 was transferred into nucleus 48 h after the infection of Ad-EGFP-C197. (A and D) C197 protein stained by TRITC-coupled antibody (red). (B and E) Cell nucleus stained by DAPI (blue). (C) A merged with B. (F) D merged with E. Magnification, x3,000. DAPI, phenylindole dihydrochloride.

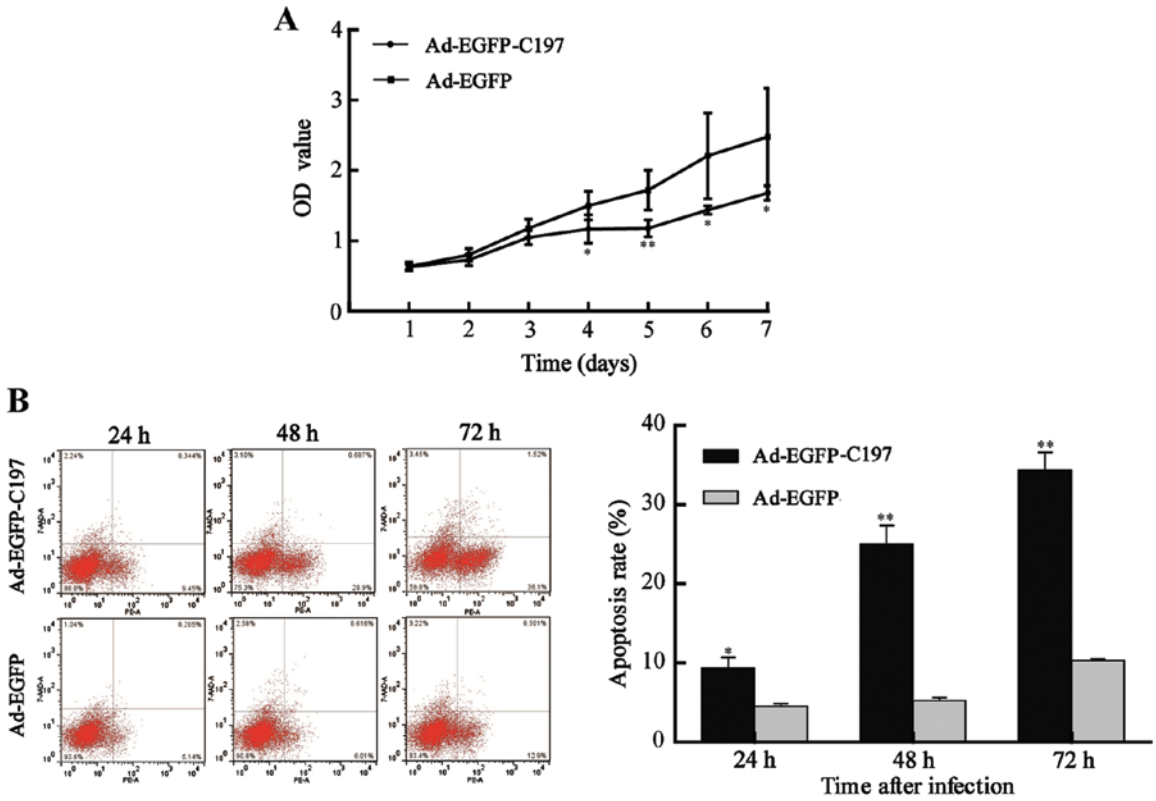

Figure 3. Ad-EGFP-C197-induced growth delay and apoptosis of HeLa cells *in vitro*. (A) Cell proliferation rate was measured by MTT. Proliferation rate was significantly lower in Ad-EGFP-C197-infected cells compared to Ad-EGFP-infected cells. (B) Quantification of apoptotic cell population (Annexin V-positive/PI-negative) by flow cytometry at 24, 48 and 72 h after infection. The apoptotic rates in Ad-EGFP-C197 infected cells were significantly higher compared to Ad-EGFP infected cells. Values are depicted as mean ± SD, n=3. *P<0.05, **P<0.01 vs. control.

after infection, respectively, P<0.05 or P<0.01, Fig. 3B), implying that apoptosis contributed to the growth inhibition induced by C197 *in vitro*.

Ad-EGFP-C197 suppresses telomerase activity and the expression of hTERT and NF-κB p65 in HeLa cells in vitro. Telomerase activity was detected by TRAP assay using

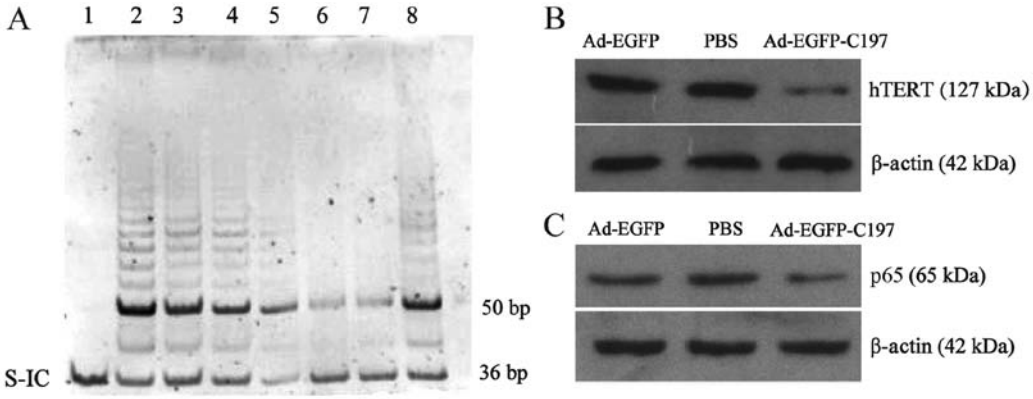

Figure 4. Ad-EGFP-C197 suppresses telomerase activity and expression of hTERT and NF-κB p65 in HeLa cells *in vitro*. (A) Ad-EGFP-C197 suppresses telomerase activity. The 36-bp internal positive control band (S-IC) is seen in every lane. Lane 1, negative control without any product except S-IC. Lane 2, telomerase-positive control cell showing a ladder of PCR products with 6 base increments starting at 50 nucleotides. Lane 3, HeLa cells infected with Ad-EGFP. Lanes 4 and 5, HeLa cells 24 and 48 h after infection with Ad-EGFP-C197, respectively. Lanes 6 and 7, HeLa cells 72 h after infection with Ad-EGFP-C197. Lane 8, HeLa cells without any treatment. (B and C) Ad-EGFP-C197 suppresses the expression of hTERT and NF-κB p65. HeLa cells were treated with Ad-EGFP, PBS or Ad-EGFP-C197. The expression of hTERT and NF-κB p65 was determined by western blot analysis. β-actin served as an internal control. hTERT, human telomerase reverse transcriptase; S-IC, standard of internal control; PBS, phosphate-buffered saline.

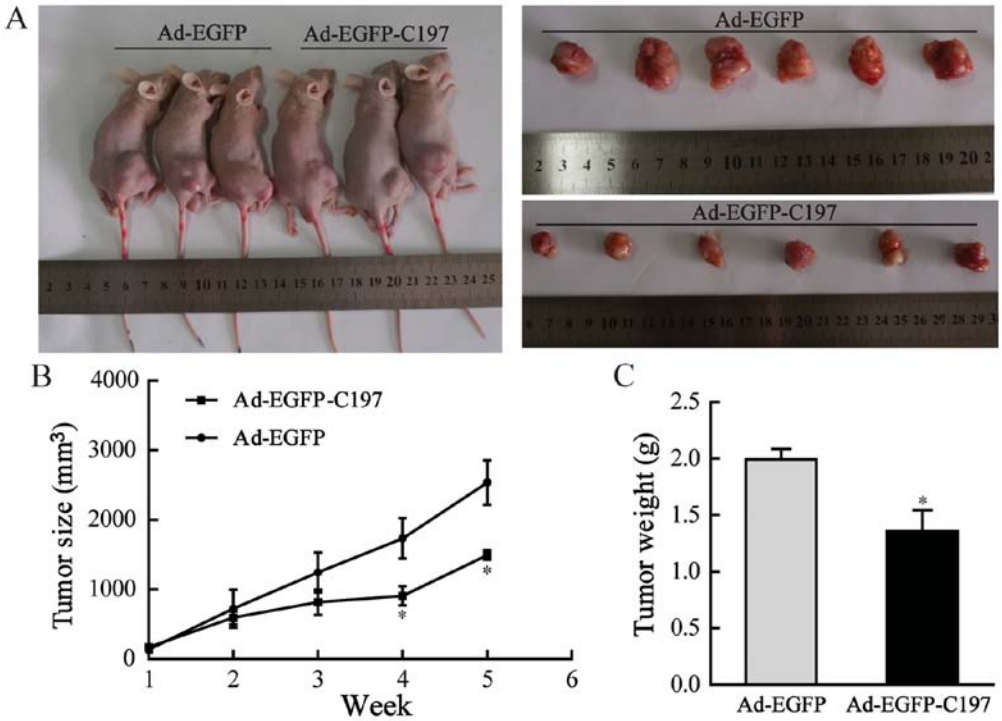

Figure 5. Ad-EGFP-C197 inhibits tumor growth *in vivo*. (A) Tumor-bearing mice and xenografted tumors were exemplarily depicted. (B and C) Tumor size and weight, respectively. Values are mean ± SD, n=6. *P<0.05 vs. Ad-EGFP.

TRAPeze kit, which generated a ladder of products with six-base increments starting at 50 nucleotides. K1 primer and TSK1 template in each reaction mixture allowed for the amplification of 36 bp nucleotides as standard of internal control (S-IC). The results (Fig. 4A) showed that telomerase activity in Ad-EGFP infected cells was unaffected when compared to untreated cells. While in cells infected with Ad-EGFP-C197, telomerase activity was significantly decreased at 48 and 72 h after infection, showing that the expression of C197 inhibited the telomerase activity in HeLa cells.

Based on the fact that hTERT is critical to the telomerase activity, we asked whether C197 affected the expression of hTERT. The results showed that infection of AD-EGFP-C197 reduced the expression of hTERT protein (Fig. 4B), which accounts for the suppressed telomerase activity.

In contrast, depressed telomerase activity impaired the telomere elongation, yet this could not explain the rapid antiproliferative effect of C197 (as shown in Fig. 2A), since there is a long lag period between the initiation of telomerase inhibition and the observing of growth arrest effect (23). Since there is a positive feedback between hTERT and NF-κB signaling pathway in the development of tumors (24), and suppression of NF-κB activation results rapidly in apoptosis in HeLa cells (25-27), we further asked whether the expression

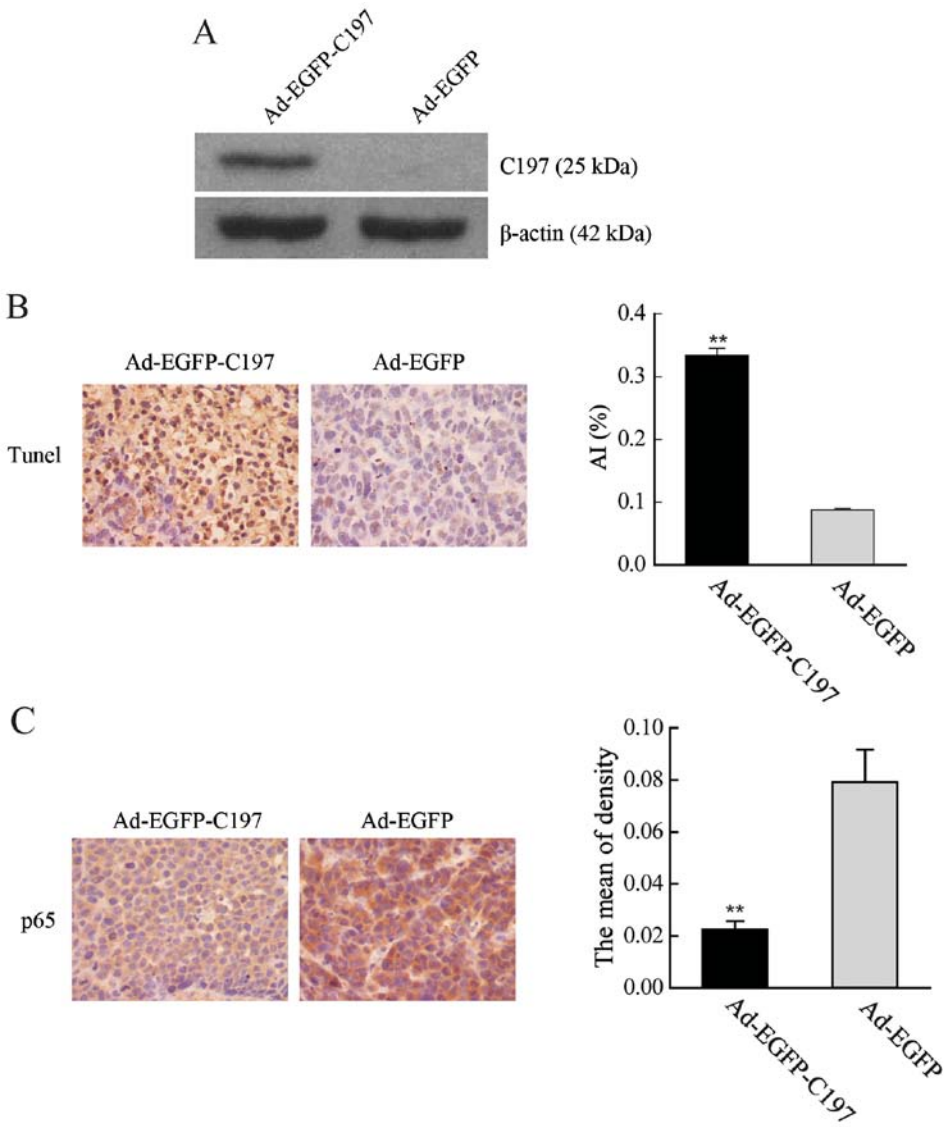

Figure 6. Ad-EGFP-C197 promotes tumor cell apoptosis and decreases expression of NF-κB p65 in tumor tissues. (A) Western blot analysis confirmed the expression of C197 in tumor tissues. β-actin served as an internal control. (B) TUNEL assays of tumor tissues to detect apoptotic cells. Magnification, x200. TUNEL-positive cells (apoptotic cells, nuclei were stained brown) and the apoptotic index (AI) were significantly higher in tumors injected with Ad-EGFP-C197 than in tumors injected with Ad-EGFP. (C) Immunohistochemistry analysis of NF-κB p65 protein (stained brown) in tumor tissues. Magnification, x200. The relative expression of NF-κB p65 protein was significantly lower in tumors injected with Ad-EGFP-C197 than in tumors injected with Ad-EGFP. Images are representative results of 3 independent experiments. Values are mean ± SD, *P<0.05, **P<0.01 compared to Ad-EGFP.

of NF-κB p65 would be affected by C197 in HeLa cells. As shown in Fig. 4C, Ad-EGFP did not affect the expression of NF-κB p65, while Ad-EGFP-C197 significantly reduced the expression of NF-κB p65 suggesting that C197 has an impact on NF-κB signaling pathway.

Ad-EGFP-C197 inhibits tumorigenicity of HeLa cells in vivo. HeLa cells were subcutaneously injected into athymic nude mice to establish xenograft tumor models, followed by injecting the resulting tumors with Ad-EGFP or Ad-EGFP-C197. Periodic measurement showed that the sizes of tumors in Ad-EGFP-C197-treated mice (909.18±309.65 mm^3 at 4 weeks, and 1496.18±153.35 mm^3 at 5 weeks) were significantly smaller than in Ad-EGFP-treated mice (1736.02±643.67 mm^3 at 4 weeks, and 2538.26±715.6 mm^3 at 5 weeks, P<0.05, Fig. 5B). At 5 weeks the weight of tumors in animals injected with Ad-EGFP-C197 (1.36±0.46 g) were significantly lower than in animals injected with Ad-EGFP (1.99±0.23 g, P<0.05, Fig. 5C).

Ad-EGFP-C197 promoted tumor cell apoptosis and decreased expression of NF-κB p65 in tumor tissues. After 4 weeks injection of Ad-EGFP-C197 or Ad-GFP, tumor tissues were subjected to TUNEL assays and immunohistochemistry analysis. In TUNEL assay, TUNEL-positive cells were more abundant in tumors injected with Ad-EGFP-C197 (AI, 0.334±0.023) than tumors injected with Ad-EGFP (AI, 0.088±0.005, P<0.01, Fig. 6B). In immunohistochemistry examination, the staining of NF-κB p65 protein was significantly lower in Ad-EGFP-C197-treated tumor tissues (MOD, 0.022±0.006) than in tissues treated with Ad-EGFP (MOD, 0.079±0.025, P<0.01, Fig. 6C).

Discussion

In the present study, we report that the ectopic expression of the novel C197 COOH-terminal polypeptide (amino acid 936-1,132) of hTERT, induced growth delay and apoptosis of HeLa cells both *in vitro* and in nude mice. Furthermore, C197 suppressed the telomerase activity which we believe was induced by the declined expression of hTERT. In contrast, previous studies showed that C27 did not affect the telomerase activity. One possible explanation of the different effects of C197 and C27 on telomerase activity is that there may be different conformations between C197 and C27, since C27 contains additional 54 amino acids (D and E conserved short motifs of reverse transcriptase domain) at the NH_2 terminus (15).

Since telomeric DNA progressively erodes at a rate of 30-120 bp with each cell cycle (28-30), there is a long lag period between the initiation of telomerase inhibition and the observing of growth arrest effect (23,31). While in the present study, C197 induced growth arrest and apoptosis of HeLa cells within a short time *in vitro* (significant effects were observed 4 days after the infection of Ad-EGFP-C197). Therefore, although telomerase activity and hTERT protein were decreased, the rapid antiproliferative effect of C197 may be independent of telomere-repairing effect of hTERT.

In the present study, ectopic expression of C197 reduced the expression of NF-κB p65, implying that C197 has an impact on NF-κB signaling pathway. NF-κB signaling pathway is known as a master regulator of cellular and developmental events and suppression of NF-κB activation results rapidly in apoptosis of HeLa cells (25-27). Although further study is needed to elucidate the mechanisms, the present data suggest that the anticancer effect of C197 is associated with the downregulation of p65 which results in the impaired function of NF-κB signaling pathway.

In recent years, it was found that hTERT and NF-κB pathway was often deregulated and overexpressed in many cancer cells, and there is a forward feedback between hTERT and NF-κB pathway (7,24). NF-κB p65 modulates hTERT expression and nuclear translocation from cytoplasm in tumor cells (32,33), and hTERT has been shown to contribute to cancer development and progression as a transcriptional modulator of the NF-κB signaling pathway in a manner independent of telomerase activity (7,8). In the present study, we speculated that the C197 interrupts the forward feedback between hTERT and NF-κB signaling pathway which contributes to the antitumor effect of C197. Reduced expression of NF-κB p65 leads to the decreased expression and activity of hTERT. In return, decreased hTERT protein in nucleus attenuates the effect of NF-κB pathway. Furthermore, it has been reported that COOH-terminus of hTERT contains binding sites for 14-3-3, a protein that prevents telomerase exporting from the nucleus (13). C197 also contains these binding sites. The present data showed that C197 was able to find its way to enter the nucleus. Nucleus accumulation of C197 binds most of 14-3-3, therefore inhibits the nuclear localization of hTERT, which further suppresses the interaction between hTERT and NF-κB pathway.

In general, our studies showed that adenovirus-mediated overexpression of C197 inhibited the growth and promoted apoptosis of HeLa cells *in vitro* and *in vivo*. Although further study is needed to elucidate the more detailed mechanisms, the present study demonstrated that the antitumor effect of C197 is associated with the downregulation of hTERT and NF-κB p65 protein. Our results, along with the previous study, suggest the potential of COOH-terminal of hTERT in the treatment of tumors.

Acknowledgements

The present study was supported by a grant from the Science and Technology Program of Guangzhou City, China (grant no. 2014J4100195).

References

1. Moyzis RK, Buckingham JM, Cram LS, Dani M, Deaven LL, Jones MD, Meyne J, Ratliff RL and Wu JR: A highly conserved repetitive DNA sequence, $(TTAGGG)_n$, present at the telomeres of human chromosomes. Proc Natl Acad Sci USA 85: 6622-6626, 1988.
2. de Lange T: Shelterin: The protein complex that shapes and safeguards human telomeres. Genes Dev 19: 2100-2110, 2005.
3. Shay JW: Telomerase therapeutics: Telomeres recognized as a DNA damage signal: Commentary re: K. Kraemer *et al*, antisense-mediated hTERT inhibition specifically reduces the growth of human bladder cancer cells. Clin Cancer Res 9: 3794-3800, 2003. Clin Cancer Res 9: 3521-3525, 2003.
4. Wright WE, Piatyszek MA, Rainey WE, Byrd W and Shay JW: Telomerase activity in human germline and embryonic tissues and cells. Dev Genet 18: 173-179, 1996.
5. Kim NW, Piatyszek MA, Prowse KR, Harley CB, West MD, Ho PL, Coviello GM, Wright WE, Weinrich SL and Shay JW: Specific association of human telomerase activity with immortal cells and cancer. Science 266: 2011-2015, 1994.
6. Low KC and Tergaonkar V: Telomerase: Central regulator of all of the hallmarks of cancer. Trends Biochem Sci 38: 426-434, 2013.
7. Ghosh A, Saginc G, Leow SC, Khattar E, Shin EM, Yan TD, Wong M, Zhang Z, Li G, Sung WK, *et al*: Telomerase directly regulates NF-κB-dependent transcription. Nat Cell Biol 14: 1270-1281, 2012.
8. Ding D, Xi P, Zhou J, Wang M and Cong YS: Human telomerase reverse transcriptase regulates MMP expression independently of telomerase activity via NF-κB-dependent transcription. FASEB J 27: 4375-4383, 2013.
9. Park JI, Venteicher AS, Hong JY, Choi J, Jun S, Shkreli M, Chang W, Meng Z, Cheung P, Ji H, *et al*: Telomerase modulates Wnt signalling by association with target gene chromatin. Nature 460: 66-72, 2009.
10. Listerman I, Gazzaniga FS and Blackburn EH: An investigation of the effects of the core protein telomerase reverse transcriptase on Wnt signaling in breast cancer cells. Mol Cell Biol 34: 280-289, 2014.
11. Li Y and Tergaonkar V: Noncanonical functions of telomerase: Implications in telomerase-targeted cancer therapies. Cancer Res 74: 1639-1644, 2014.
12. Autexier C and Lue NF: The structure and function of telomerase reverse transcriptase. Annu Rev Biochem 75: 493-517, 2006.
13. Seimiya H, Sawada H, Muramatsu Y, Shimizu M, Ohko K, Yamane K and Tsuruo T: Involvement of 14-3-3 proteins in nuclear localization of telomerase. EMBO J 19: 2652-2661, 2000.
14. Banik SS, Guo C, Smith AC, Margolis SS, Richardson DA, Tirado CA and Counter CM: C-terminal regions of the human telomerase catalytic subunit essential for in vivo enzyme activity. Mol Cell Biol 22: 6234-6246, 2002.
15. Huang JJ, Lin MC, Bai YX, Jing DD, Wong BC, Han SW, Lin J, Xu B, Huang CF and Kung HF: Ectopic expression of a COOH-terminal fragment of the human telomerase reverse transcriptase leads to telomere dysfunction and reduction of growth and tumorigenicity in HeLa cells. Cancer Res 62: 3226-3232, 2002.
16. Ng SS, Gao Y, Chau DH, Li GH, Lai LH, Huang PT, Huang CF, Huang JJ, Chen YC, Kung HF, *et al*: A novel glioblastoma cancer gene therapy using AAV-mediated long-term expression of human TERT C-terminal polypeptide. Cancer Gene Ther 14: 561-572, 2007.

17. Gao Y, Ng SS, Chau DH, Yao H, Yang C, Man K, Huang PT, Huang C, Huang JJ, Kung HF, *et al*: Development of recombinant adeno-associated virus and adenovirus cocktail system for efficient hTERTC27 polypeptide-mediated cancer gene therapy. Cancer Gene Ther 15: 723-732, 2008.
18. He L, Gong HX, Li XP, Wang YD, Li Y, Huang JJ, Xie D, Kung HF and Peng Y: Inhibition of hepatocellular carcinoma growth by adenovirus-mediated expression of human telomerase reverse transcriptase COOH-27 terminal polypeptide in mice. Oncol Lett 6: 748-752, 2013.
19. Huo L, Yao H, Wang X, Wong GW, Kung HF and Lin MC: Inhibition of melanoma growth by subcutaneous administration of hTERTC27 viral cocktail in C57BL/6 mice. PLoS One 5: e12705, 2010.
20. Lin G, Chen Q, Yu S, Lin S, Yao H, Ding Z, Chen S, Lin MC and Wang X: Overexpression of human telomerase reverse transcriptase C-terminal polypeptide sensitizes HeLa cells to 5-fluorouracil-induced growth inhibition and apoptosis. Mol Med Rep 9: 279-284, 2014.
21. Li HW, Gao YX, Raizada MK and Sumners C: Intronic enhancement of angiotensin II type 2 receptor transgene expression in vitro and in vivo. Biochem Biophys Res Commun 336: 29-35, 2005.
22. Yoon JW, Lee JS, Kim BM, Ahn J and Yang KM: Catechin-7-O-xyloside induces apoptosis via endoplasmic reticulum stress and mitochondrial dysfunction in human non-small cell lung carcinoma H1299 cells. Oncol Rep 31: 314-320, 2014.
23. Damm K, Hemmann U, Garin-Chesa P, Hauel N, Kauffmann I, Priepke H, Niestroj C, Daiber C, Enenkel B, Guilliard B, *et al*: A highly selective telomerase inhibitor limiting human cancer cell proliferation. EMBO J 20: 6958-6968, 2001.
24. Wu XQ, Huang C, He X, Tian YY, Zhou DX, He Y, Liu XH and Li J: Feedback regulation of telomerase reverse transcriptase: new insight into the evolving field of telomerase in cancer. Cell Signal 25: 2462-2468, 2013.
25. Lu W, Zhang G, Zhang R, Flores LG II, Huang Q, Gelovani JG and Li C: Tumor site-specific silencing of NF-kappaB p65 by targeted hollow gold nanosphere-mediated photothermal transfection. Cancer Res 70: 3177-3188, 2010.
26. Li Y, Xing D, Chen Q and Chen WR: Enhancement of chemotherapeutic agent-induced apoptosis by inhibition of NF-kappaB using ursolic acid. Int J Cancer 127: 462-473, 2010.
27. Juneja M, Vanam U, Paranthaman S, Bharathan A, Keerthi VS, Reena JK, Rajaram R, Rajasekharan KN and Karunagaran D: 4-Amino-2-arylamino-5-indoloyl/cinnamoythiazoles, analogs of topsentin-class of marine alkaloids, induce apoptosis in HeLa cells. Eur J Med Chem 63: 474-483, 2013.
28. Harley CB, Futcher AB and Greider CW: Telomeres shorten during ageing of human fibroblasts. Nature 345: 458-460, 1990.
29. Hastie ND, Dempster M, Dunlop MG, Thompson AM, Green DK and Allshire RC: Telomere reduction in human colorectal carcinoma and with ageing. Nature 346: 866-868, 1990.
30. Counter CM, Avilion AA, LeFeuvre CE, Stewart NG, Greider CW, Harley CB and Bacchetti S. Telomere shortening associated with chromosome instability is arrested in immortal cells which express telomerase activity. EMBO J 11, 1921-1929, 1992.
31. Hahn WC, Stewart SA, Brooks MW, York SG, Eaton E, Kurachi A, Beijersbergen RL, Knoll JH, Meyerson M and Weinberg RA: Inhibition of telomerase limits the growth of human cancer cells. Nat Med 5: 1164-1170, 1999.
32. Zuo QP, Liu SK, Li ZJ, Li B, Zhou YL, Guo R and Huang LH: NF-kappaB p65 modulates the telomerase reverse transcriptase in the $HepG_2$ hepatoma cell line. Eur J Pharmacol 672: 113-120, 2011.
33. Akiyama M, Hideshima T, Hayashi T, Tai YT, Mitsiades CS, Mitsiades N, Chauhan D, Richardson P, Munshi NC and Anderson KC: Nuclear factor-kappaB p65 mediates tumor necrosis factor alpha-induced nuclear translocation of telomerase reverse transcriptase protein. Cancer Res 63: 18-21, 2003.